Reliable femoral frame construction based on MRI dedicated to muscles position follow-up

G. Dubois[1] · D. Bonneau[1] · V. Lafage[2] · P. Rouch[1] · W. Skalli[1]

Abstract In vivo follow-up of muscle shape variation represents a challenge when evaluating muscle development due to disease or treatment. Recent developments in muscles reconstruction techniques indicate MRI as a clinical tool for the follow-up of the thigh muscles. The comparison of 3D muscles shape from two different sequences is not easy because there is no common frame. This study proposes an innovative method for the reconstruction of a reliable femoral frame based on the femoral head and both condyles centers. In order to robustify the definition of condylar spheres, an original method was developed to combine the estimation of diameters of both condyles from the lateral antero-posterior distance and the estimation of the spheres center from an optimization process. The influence of spacing between MR slices and of origin positions was studied. For all axes, the proposed method presented an angular error lower than 1° with spacing between slice of 10 mm and the optimal position of the origin was identified at 56 % of the distance between the femoral head center and the barycenter of both condyles. The high reliability of this method provides a robust frame for clinical follow-up based on MRI .

Keywords Femoral frame · MRI · Muscle · Thigh

1 Introduction

Muscle shape variation is an important factor for studying the effects of age, neuromuscular pathology or treatment. In vivo follow-up of muscle shape variation is a great challenge in clinical patients in order to evaluate muscle development from disease or treatment [14, 22]. Muscle volume variation is investigated from reduced cross-sectional area [13, 16, 23] or from 3D muscle reconstruction which is more accurate. Muscle volume is commonly evaluated using axis slices from magnetic resonance images (MRIs) [5, 17] or CT-Scan [10, 18, 19]. The 3D muscle shape is accessed by manual segmentation of the whole muscles contours. Some recent studies presented improvement in the reconstruction method in order to decrease the reconstruction time by decreasing the number of segmented slices [10, 21] or by automating the segmentation [6].

However, assessing volume evolution of muscle belly is still a challenge. A previous study has shown that the inter-operator reliability for the muscle volume evaluation ranged from 2 to 11 % depending on the muscles of the thigh [21]. These differences were due to the difficulty of identifying the muscle belly, and of choosing the upper and lower slices of one muscle. Our group proposed to define a local coordinate system in order to locate the upper and lower slices part of the muscle belly and to get a stable reference during follow-up. This increased the trustworthiness of muscles volume comparison by defining muscles limits more accurately.

The definition of a reliable femoral frame is also a challenge in gait analysis to efficiently quantify the angular position between the anatomical segments. Several studies proposed the use of the femoral frame [1, 2, 4], but the recommendation of the International Society of Biomechanics (ISB) is assumed as the reference [25]. As a result, the frame should be defined with the femur head center and the

points represented by the medial and lateral epicondyles. However, these two points are visible on MRI slices only if the femur is cut at the right height and hence this method is difficult to use without using 3D reconstruction. In order to combine thigh muscles from MRI [10] and femur from biplanar X-ray [3] in the same coordinate system, authors proposed to use the femoral head center and the medial and distal condylar centers [8]. A difficult issue in this process is to locate the center of the condyles because they appeared as small arcs on few MRI slices.

These points have been used to define the axis orientation and the origin. ISB recommendation and Hausselle et al. [8] assumed the femoral head center as the origin of the femoral frame. In movement analysis, femoral head center is estimated using functional methods [20]. But to our knowledge, no evaluation of the reliability of the femoral head center has been performed on MRI. In order to identify more precisely the upper and lower slices of muscles, the origin had to be defined as the most reliable point in the frame.

The aim of the proposed method is to define and to evaluate the reliability of a femoral frame based on MRI in order to study the variation of the muscle position in clinical routine. The optimal location of the origin position was also studied.

2 Materials and method

In order to locate the upper (UpS) and lower (LwS) slices of muscle belly, a femoral frame was constructed and the best position of the origin (O) was investigated to locate UpS and LwS with the lowest possible error (Fig. 1).

2.1 Femoral frame definition

The three spheres centers defined by the femoral head (F_h) , the lateral condyle (L_c) and the medial condyle (M_c) have been chosen to construct the femoral frame (Fig. 1). Z axis was defined along the line passing through the middle of both condylar center spheres (M) and F_h (Eq. 1). $\overrightarrow{X}$ axis was defined as the normal vector of the plane passing through F_h, M_c and L_c (Eq. 2). $\overrightarrow{Y}$ axis was defined as the cross product of $\overrightarrow{Z}$ axis and $\overrightarrow{X}$ axis (Eq. 3). The femoral head center defined the femoral frame origin.

$$\overrightarrow{Z} = \frac{\overrightarrow{MF_\mathrm{h}}}{\left\|\overrightarrow{MF_\mathrm{h}}\right\|} \tag{1}$$

$$\overrightarrow{X} = \frac{\overrightarrow{L_\mathrm{c}M_\mathrm{c}} \wedge \overrightarrow{Z}}{\left\|\overrightarrow{L_\mathrm{c}M_\mathrm{c}} \wedge \overrightarrow{Z}\right\|} \tag{2}$$

$$\overrightarrow{Y} = \overrightarrow{Z} \wedge \overrightarrow{X} \tag{3}$$

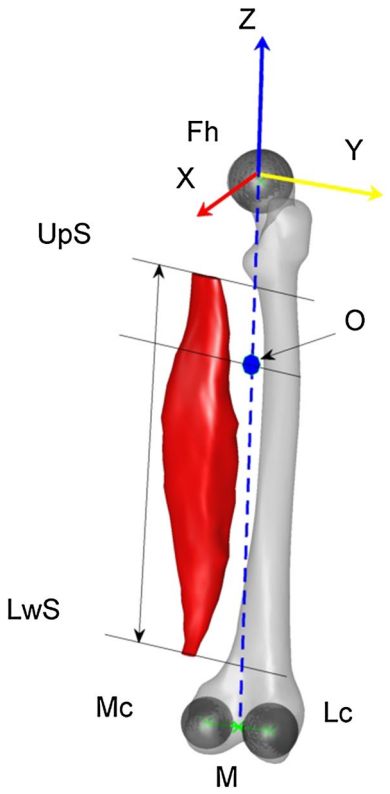

Fig. 1 Femoral frame computed from the femoral head center (F_h), the medial condyle (M_c) and the lateral condyle (L_c). $\overrightarrow{X}$ axis in red, $\overrightarrow{Y}$ axis in yellow and $\overrightarrow{Z}$ in blue. Muscle belly was defined between the upper (UpS) and lower (LwS) slices (color figure online)

2.2 Computation of the femoral sphere

The femoral head was recognizable on MRI slices as a set of circle of around 5 mm thick (cortical bone) (Fig. 2). The operator selected manually a minimum of 10 points equally spaced in each slice corresponding to the extremity of the femoral head. Then, the sphere associated with the point cloud was computed with a least squares method.

2.3 Definition of the condylar spheres

The condyles appeared as a set of small arcs on only few slices (3–4 slices) (Fig. 2), which makes it difficult to assess the spheres diameters and to position them. Therefore, a correlation study based on femoral database was made to estimate the spheres diameters. Then, an optimization process was used to assess the spheres centers.

2.3.1 Computation of the condylar spheres diameter

A database of 26 non-pathologic femurs reconstructed from manual segmentation on CT-Scan was used. The Pearson's coefficients showed that the lateral and medial condyles

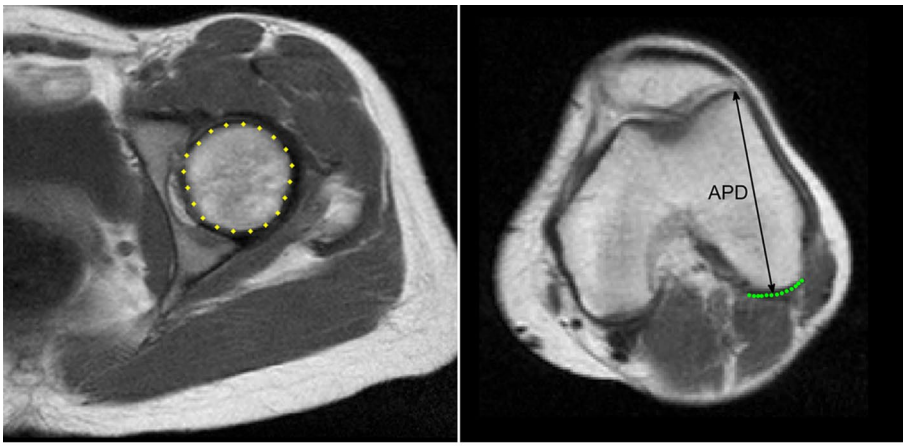

Fig. 2 Segmentation of the femoral head and lateral condyle on MRI and selection of the antero-posterior distance on the lateral condyle

diameter (L_cD and M_cD) can be estimated from the antero-posterior distance of the lateral condyle ($r_{L_cD} = 0.90$, $p < 0.001$ and $r_{M_cD} = 0.68$, $p < 0.001$) or from the antero-posterior distance of the medial condyle ($r_{L_cD} = 0.86$, $p < 0.001$ and $r_{M_cD} = 0.73$, $p < 0.001$). The estimation was only based on the antero-posterior distance of the lateral condyle (APD), which was more easy and reliable to select (Fig. 2) and in order to limit the selection to one distance.

Uncertainty of diameters estimation was assessed using a Leave One Out (LOO) method. For each subject, S_i, L_cD and M_cD were computed from a linear regression on sample from the database excluding S_i. The error was defined as the difference between estimated value of the diameters ($L_cD_{\text{est},i}$, $M_cD_{\text{est},i}$) and their real diameters ($L_cD_{\text{real},i}$, $M_cD_{\text{real},i}$). For L_cD and M_cD, the mean of the absolute value of the errors was computed (Eqs. 4, 5).

$$e_{\text{LOO}} = \frac{1}{n}\sum_{i=1}^{n}\left|L_cD_{\text{est},i} - L_cD_{\text{real},i}\right| \tag{4}$$

$$e_{\text{LOO}} = \frac{1}{n}\sum_{i=1}^{n}\left|M_cD_{\text{est},i} - M_cD_{\text{real},i}\right| \tag{5}$$

The linear regression equation was defined on the whole sample, and the standard errors of the estimate (SEE) were computed (Eqs. 6, 7).

$$\text{SEE} = \sqrt{\frac{1}{n}\sum_{i=1}^{n}\left(L_cD_{\text{est},i} - L_cD_{\text{real},i}\right)^2} \tag{6}$$

$$\text{SEE} = \sqrt{\frac{1}{n}\sum_{i=1}^{n}\left(M_cD_{\text{est},i} - M_cD_{\text{real},i}\right)^2} \tag{7}$$

For the lateral condyle, the regression equation was $r_{L_cD} = 0.47\text{APD} + 8.28$, $e_{\text{LOO}} = 2.01\,\text{mm}$ and $\text{SEE} = 2.32\,\text{mm}$. For the medial condyle diameter, the line equation was $r_{L_cD} = 0.83\text{APD} - 11.88$, $e_{\text{LOO}} = 1.37\,\text{mm}$ and $\text{SEE} = 1.77\text{mm}$.

The presented regression equations were implemented in order to estimate L_cD and M_cD.

2.3.2 Positioning of the condylar spheres

Once the condylar spheres diameters were calculated, a two-step process was defined for their positioning. The location of the spheres centers was approximated in order to initialize the optimization algorithm, and finally, the position was optimized:

1. First estimate of spheres centers:
   (a) The operators selected at least five points distributed on each slice which represent the small arcs of the condyles, and these points (M) are considered as belonging to the condylar sphere. To assess the sphere center, the following property was considered: Each segment of two points from M has a bisector plane passing through the sphere center.
   (b) Fifty different planes P_k were defined (Fig. 3a): Two randomized points $M_i \in M$ and $M_j \in M$ were selected with a distance constraint between them (e.g., spacing between slices). A plane P_k was defined passing through the middle of M_i and M_j, noted P_{M_k} and having as normal the vector $\overrightarrow{P_{N_k}} = \overrightarrow{M_iM_j}$.
   (c) The intersection between three different planes provided a point I_m, theoretical location of the sphere center. The combination of three planes

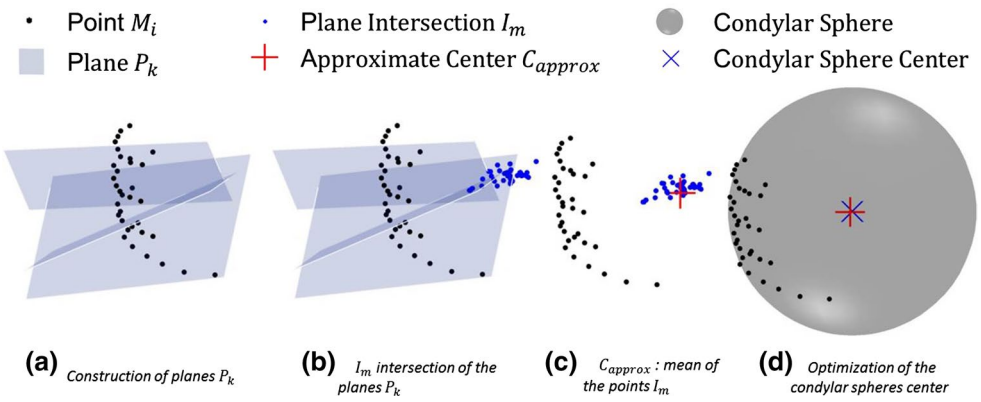

Fig. 3 Points M_i were identified by the operator, then the mean (C_{approx}) of the intersections I_m of the planes P_k gave the first approximation of the condylar sphere center

P_l, P_m, P_n should respect a criteria: The distance between the middle of the segments defining the three planes P_{M_l}, P_{M_m}, P_{M_n} must be higher than a minimal value (e.g., spacing between slices).
Fifty points I_m were constructed (Fig. 3b) by a random combination of planes P_k satisfying the above criteria. A check was performed to avoid possible quasi coplanar planes $\det(P_{N_i}, P_{N_j}, P_{N_k}) > 10^{-3}$ and a combination of two planes was used only once.

(d) The mean of the 50 resulting points I_m gave an approximate position of the sphere center C_{approx} (Fig. 3c).

2. The sphere center position was optimized from C_{approx} and the estimate radius, by the iterative Gauss-Newton algorithm, in order to minimize the distance between the points M and the sphere (Fig. 3d).

In order to assess the advantage of a such method, the least squares spheres were also computed.

2.4 Subjects

Five female subjects with no documented muscular pathology (age: 59 ± 12.7 years, weight: 55 ± 11.3 kg, height: 156 ± 7.7 cm) agreed to participate in this protocol approved by the institutional ethics committee.

MRI was performed on a 3T whole-body scanner from the iliac crests to the tibial plateau (Magnetom Skyra, Siemens Healthcare, Erlangen, Germany) using a 24-channel spine matrix coil and three 16-channel flex coils from the same vendor (3D acquisition, TR/TE = 820/11 ms, acquisition matrix = 448 × 308, phase oversampling = 100 %, in plane resolution = 0.94 mm^2, 4 stages, 40 slices by stage, slice thickness = 5 mm, slice gap= 0 mm, flip angle = 157°, turbo factor = 3, echo trains = 107, parallel imaging acceleration factor (iPat) = 2, iPat references lines = 26, bandwidth = 319 Hz/pixel, echo spacing = 15.7, acquisition time per stage = 5:53 min, total acquisition time = 25 min).

2.5 Reliability study

In order to assess the intra- and inter-operator reliability, the method was performed five times by two operators on five subjects. For each reconstruction (i.e., 10 per subject), the rotation angles between the global coordinate system of the MRI device and the femoral coordinate system were computed with the mobile angle sequence $XY'Z''$. Then, the mean values were considered as a reference and each specific value was compared to the reference one. The intra- and inter-operator reliability was computed using the ISO 5725 Standard.

2.6 Slice number influence

The influence of the number of segmented slices was investigated. The spacing between slices (SBS) was of 5 mm for all subjects, and both condyles were visible on 3–4 slices and the femoral on 5–7 slices. By dividing the number of slices by 2, an MRI sequence with a SBS of 10 mm was created. The reliability study was realized on both sequences.

2.7 Influence of the origin on muscles position reliability

The following 12 muscles involved in knee motion were studied according to previous studies and functional considerations [12, 15, 21]: semimembranosus (SM), semitendinosus (ST), biceps femoris long head (BFL), biceps femoris short head (BFS), sartorius (SAR), tensor fascia latae (TFL), gracilis (GRA), vastus lateralis and vastus intermedius (VIL), vastus medialis (VM), rectus femoris (RF), medial gastrocnemius (MG), and lateral gastrocnemius (LG). For all muscles, UpS and LwS corresponding to the muscle belly were investigated. UpS and LwS were located in the uniaxial frame with a direction along the Z axis of the origin (Fig. 1).

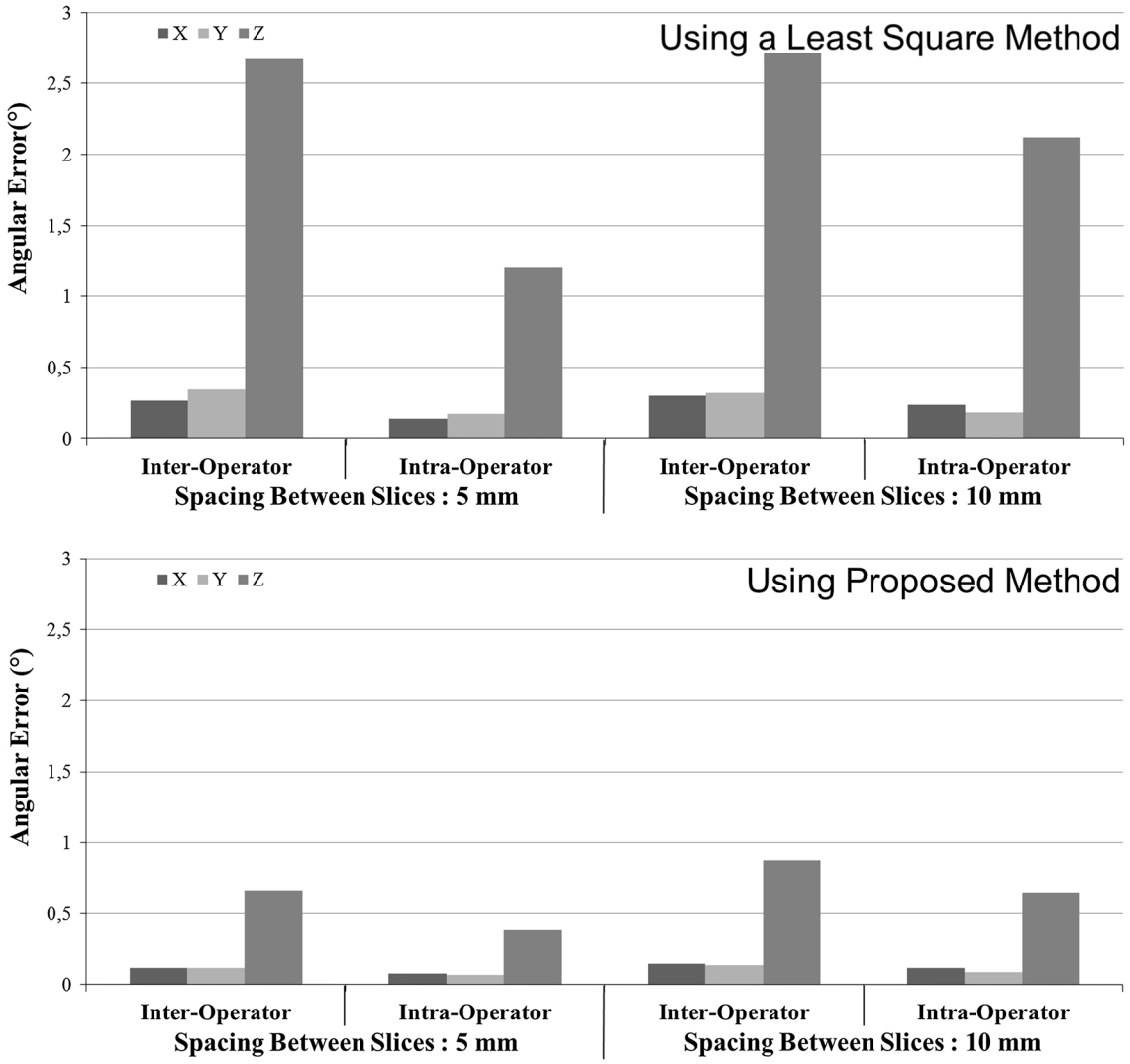

Fig. 4 Inter- and intra-operator angular error along $\overrightarrow{X}$, $\overrightarrow{Y}$ and $\overrightarrow{Z}$ axis by varying SBS from 5 to 10 mm for the proposed method and the least squares method

In order to quantify the influence of origin position of the frame on the muscle extremity position reliability, the inter-operator reliability errors along the Z axis were computed for all UpS and LwS by varying the origin from the femoral head center to both condyles barycenters. For the least squares method and the proposed method, the mean of the error was studied by varying SBS from 5 to 10 mm.

3 Results

3.1 Frame reliability

- With a least squares method, the inter-operator error varied from 0.27° to 2.7° and the intra-operator error varied from 0.13° to 0.21° (Fig. 4). An increase of approximately 0.5°, 0.2° and 0.9° was, respectively, observed on $\overrightarrow{X}$, $\overrightarrow{Y}$ and $\overrightarrow{Z}$ axis when the SBS increased from 5 to 10 mm.
- With the proposed method, the inter-operator error varied from 0.1° to 0.9° and the intra-operator error varied from 0.08° to 0.7° (Fig. 4). An increase of approximately 0.03°, 0.03° and 0.26° was, respectively, observed on $\overrightarrow{X}$, $\overrightarrow{Y}$ and $\overrightarrow{Z}$ axis when the SBS increased from 5 to 10 mm. All errors in all cases remained lower than 1°.

3.2 Muscles position reliability

The mean of the 11 muscles positions reproducibility was similar for both methods. SBS affected more significantly the error (Fig. 5).

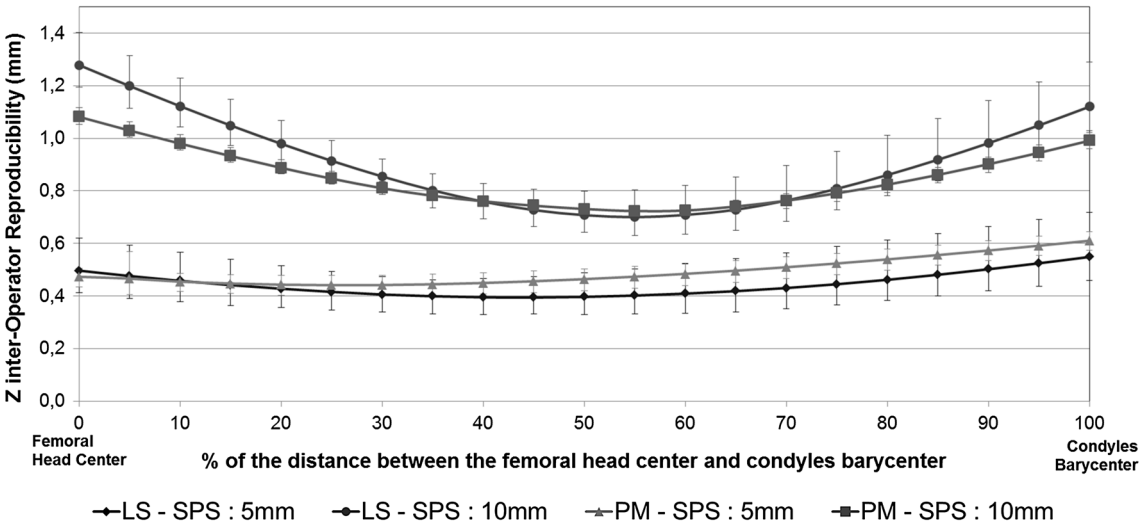

Fig. 5 Mean of 11 muscles position reproducibility by varying origin position from the femoral head center to condyles barycenter for the least squares method (LS) and the proposed method (PM) by varying SBS from 5 to 10 mm

- With a SBS of 5 mm, the lowest error appeared around 50 % for the least squares method with an error of 0.4 mm and at 20 % for the proposed method with an error of 0.5 mm. Considering origin between 0–50 % of the distance between the femoral head center and the barycenter of both condyles induced an error around 0.1 mm.
- With a SBS of 10 mm, the lowest error appeared around 55 % for both methods with an error of 0.72 mm. Considering the femoral head center as origin induced an error of 1.3 mm.

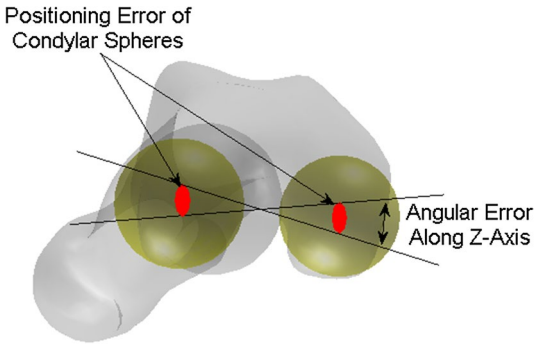

Fig. 6 Angular error due to positioning errors of sphere centers from diameter estimation error

4 Discussion

The aim of the proposed method was to develop a simple reliable method to construct a femoral frame based on MRI. The difficulty was to identify three reproducible points in order to position the frame. The femoral head was an evident choice by its ease of identification and positioning. Both condylar spheres were visible on numerous frames; their centers were already used for the construction of the femoral frame [8]. However, they appeared as small arcs, their positions were not reliable with the least squares method and, indeed, an inter-operator error along the $\overrightarrow{Z}$ axis of 2.5° was found with SBS of 5 mm. A new approach was used by estimating the spheres diameters from correlation with a maximum error of 10 % on the diameter. Given geometric considerations, estimation error could yield a rotation error of 1.2° along the $\overrightarrow{Z}$ axis (Fig. 6). This error was the same for all reconstructions; this static error did not affect the frame reliability and was not significant. Then, an inter-operator error along the Z axis of 0.7° was found with SBS of 5 mm.

The angular error was more important on the $\overrightarrow{Z}$ axis. The distance between both condyles was about 40 mm, and the distance between condyles and femoral head center is about 400 mm. The positioning error of the condyles and femoral head centers is about 5 mm. Thus, the positions of the $\overrightarrow{X}$ and $\overrightarrow{Y}$ axis are most sensitive to the positioning error than $\overrightarrow{Z}$ axis. The frame was most influenced by the positioning of the condylar spheres on the ($\overrightarrow{X}$, $\overrightarrow{Y}$) plane. The arcs, where the condyles were visible, were very small; the displacement of one point modified the position of the spheres. However, this variation only induced an angular error inferior to 1°, which all remained even with 10 mm SBS.

The operator always selected the points on the same slices; thus, all the points were always on the same Z level. In order to quantify this effect, the following study was performed. For all subjects where the condyles were visible on 4 slices, the reliability study was performed on

both sequences of 10 mm and no positioning influence was found.

The intra-operator error was found to be less than the inter-operator error. Each operator has selected points with a good reliability, but the selection was different between operators. No specification was given for points selection on the cortical bone. Its thickness was measured as approximately 3 mm; some operators selected points on the exterior and some other on the middle part. Automation should increase the method reliability. As proposed by Jolivet et al. [11], the use of a gradient, pixel intensity and distance cost function should allow detecting the interface between bone and articular capsule.

The SBS influenced less the inter-operator reliability than the intra-operator with an increasing of 28 % against 75 %. For the same operator, the use a SBS of 5 mm increased significantly the reliability of the frame. The number of contours for the condylar spheres was multiplied by 1.5 or by 2, and it allowed to position them better. Nevertheless, increase in uncertainty did not affect significantly the reliability, since the Z-inter-operator reliability error was only 0.65° to 0.87°.

While femoral frame assessment was used in various studies from CT-Scan or MRI [7, 9, 24], very few of them addressed the issue of its reliability. Furthermore, frames are identified from landmarks noticeable on 3D reconstructions which require a large number of slices. Nevertheless, the posterior condylar line reliability was assessed by an intra-operator angular error of 0.16° and an inter-operator angular error of 0.57°, corresponding to the $\overrightarrow{Z}$ axis angular error and their results were closed to ours [24]. To our knowledge, this is the first study addressing a reliable femoral frame based on MRI, indeed, because of the lack of visibility on MRI and the reduced number of slices in routine clinical analysis. Condyles assessment using least squares best fit spheres gave low reliability; the proposed method provided a reliable alternative.

The femoral head position was more reliable than that of the condyles; the definition of the origin was a major factor in order to decrease the positioning error of each muscle extremity inside the femoral frame. For all muscles, the more reliable position was included 10–20 % of the distance between the femoral head center and the barycenter of both condyles from the femoral head center with SBS of 5 mm. At 15 %, the average error was minimal and the variation was less than 0.03 mm under 40 %. Then, an approximation had to be done by considering the femoral head as origin for the proposed method. Thus, the upper and the lower slices could be expressed inside the proposed femoral frame with a $\overrightarrow{Z}$ error lower than 0.65 mm for each muscle. For a SBS of 10 mm, the approximation could not be done, and then the origin had to be chosen at 55 % of the distance. At this position, the average error was around 0.75 mm. SBS had a major effect on upper and lower slices location, using SBS of 5 mm significantly decreases the positioning error by 2 when the femoral head was considered as origin.

The correlation was computed on a database of 26 non-pathologic subjects. The method was well evaluated on five healthy subjects. The relation between the antero-posterior distance of the lateral condyle and condyles diameters has to be confirmed on pathologic subject and could be different, for example in deforming pathologies such as CP. However, the correlation was used to estimate condyles diameters. The comparison of two reconstructions at different times should not be affected with a less accurate evaluation of the diameters. Indeed, the frame should be reconstructed with the same error, which was evaluated in the present paper. Accuracy of the registration of two frames could me more questionable.

This work highlighted the potential of the correlation used to estimate parameters for frame reconstructions. The main difficulty was to identify reliable points even when the slices positioning were variable. The use of spheres increased the accuracy of anatomical landmarks identification. Thus, this could be integrated to hip frame reconstruction, using the centers of acetabulum and the sacral plane. A correlation could be used to better orientate it. The positioning of the tibial frame is more difficult: Computation of spheres is not easy. The middles of regions such as medial plateau, lateral plateau and the malleolus could be used to compute the orientation, and a correlation between femur and tibia could be used to locate the center of the tibial frame.

The proposed method has shown a high reliability with SBS of 5 mm. One of the major advantage of this method is to provide an estimate of muscle volume independent of the operator or slices positioning between two MRI sequences for the patient follow-up. Indeed, on the first MRI sequence the operator segments thigh muscles and constructs the femoral frame with the proposed method. Upper and lower slices location are given in femoral frame with a positioning error of 0.6 mm. Then, on the second MRI sequence, an operator segments the same muscles and constructs the femoral frame. In order to compare muscle volume between both MRI sequence, muscle volume are computed at the same Z level: between the level of the upper and lower slices based on the first MRI sequences. By adding the positioning error on both MRI sequence, upper and lower slices are defined with a maximum error of 1.2 mm. This locating error induces a volume error from 0.1 % for the BFS to 1 % for the SM. This error is of the same order as the reconstruction error induced by an operator. This method provides an accurate method for the patient follow-up based on MRI.

Acknowledgments The authors would like to thank Bertrand Moal for his contribution.

References

1. Besier TF, Sturnieks DL, Alderson JA, Lloyd DG (2003) Repeatability of gait data using a functional hip joint centre and a mean helical knee axis. J Biomech 36(8):1159–1168
2. Cappozzo A, Catani F, Croce UD, Leardini A (1995) Position and orientation in space of bones during movement: anatomical frame definition and determination. Clin Biomech 10(4):171–178
3. Chaibi Y, Cresson T, Aubert B, Hausselle J, Neyret P, Hauger O, de Guise JA, Skalli W (2012) Fast 3D reconstruction of the lower limb using a parametric model and statistical inferences and clinical measurements calculation from biplanar X-rays. Comput Methods Biomech Biomed Eng 15(5):457–466
4. Croce UD, Camomilla V, Leardini A, Cappozzo A (2003) Femoral anatomical frame: assessment of various definitions. Med Eng Phys 25(5):425–431
5. Eng CM, Abrams GD, Smallwood LR, Lieber RL, Ward SR (2007) Muscle geometry affects accuracy of forearm volume determination by magnetic resonance imaging (MRI). J Biomech 40(14):3261–3266
6. Gilles B, Magnenat-Thalmann N (2010) Musculoskeletal MRI segmentation using multi-resolution simplex meshes with medial representations. Med Image Anal 14(3):291–302
7. Gilles B, Perrin R, Magnenat-Thalmann N, Vallee JP (2005) Bone motion analysis from dynamic MRI: acquisition and tracking 1. Acad Radiol 12(10):1285–1292
8. Hausselle J, Assi A, El Helou A, Jolivet E, Pillet H, Dion E, Bonneau D, Skalli W (2014) Subject-specific musculoskeletal model of the lower limb in a lying and standing position. Comput Methods Biomech Biomed Eng 17(5): 480–487
9. Hemmerich A, van der Merwe W, Vaughan C (2009) Measuring three-dimensional knee kinematics under torsional loading. J Biomech 42(2):183–186
10. Jolivet E, Daguet E, Pomero V, Bonneau D, Laredo JD, Skalli W (2008) Volumic patient-specific reconstruction of muscular system based on a reduced dataset of medical images. Comput Methods Biomech Biomed Eng 11(3):281–290
11. Jolivet E, Dion E, Rouch P, Dubois G, Charrier R, Payan C, Skalli W (2014) Skeletal muscle segmentation from MRI dataset using a model-based approach. Comput Methods Biomech Biomed Eng Imaging Vis 2(3): 138–145
12. Lloyd DG, Besier TF (2003) An EMG-driven musculoskeletal model to estimate muscle forces and knee joint moments in vivo. J Biomech 36(6):765–776
13. Lund H, Christensen L, Savnik A, Boesen J, Danneskiold-Samse B, Bliddal H (2002) Volume estimation of extensor muscles of the lower leg based on MR imaging. Eur Radiol 12(12):2982–2987
14. Mendiguchia J, Garrues MA, Cronin JB, Contreras B, Arcos AL, Malliaropoulos N, Maffulli N, Idoate F (2013) Non-uniform changes in MRI measurements of the thigh muscles following two hamstring strengthening exercises. J Strength Cond Res 27(3):574–581
15. Mikosz RP, Andriacchi TP, Andersson GBJ (1988) Model analysis of factors influencing the prediction of muscle forces at the knee. J Orthop Res 6(2):205–214
16. Morse C, Degens H, Jones D (2007) The validity of estimating quadriceps volume from single MRI cross-sections in young men. Eur J Appl Physiol 100(3):267–274
17. Ng H, Ong S, Liu J, Huang S, Foong K, Goh P, Nowinski W (2009) 3D segmentation and quantification of a masticatory muscle from MR data using patient-specific models and matching distributions. J Digit Imaging 22(5):449–462
18. Overend TJ, Cunningham DA, Paterson DH, Lefcoe MS (1992) Thigh composition in young and elderly men determined by computed tomography. Clin Physiol 12(6):629–640
19. Rice CL, Cunningham DA, Paterson DH, Lefcoe MS (1989) Arm and leg composition determined by computed tomography in young and elderly men. Clin Physiol 9(3):207–220
20. Sangeux M, Pillet H, Skalli W (2014) Which method of hip joint centre localisation should be used in gait analysis? Gait Posture 40(1):20–5
21. Sudhoff I, de Guise JA, Nordez A, Jolivet E, Bonneau D, Khoury V, Skalli W (2009) 3D-patient-specific geometry of the muscles involved in knee motion from selected MRI images. Med Biol Eng Comput 47(6):579–587
22. ten Dam L, van der Kooi A, van Wattingen M, de Haan R, de Visser M (2012) DP 21 reliability and accuracy of skeletal muscle imaging in limb girdle muscular dystrophies. Neuromuscul Disord 22(9–10):824
23. Tracy BL, Ivey FM, Hurlbut D, Martel GF, Lemmer JT, Siegel EL, Metter EJ, Fozard JL, Fleg JL, Hurley BF (1999) Muscle quality. II. Effects of strength training in 65- to 75-yr-old men and women. J Appl Physiol 86(1):195–201
24. Victor J, Van Doninck D, Labey L, Van Glabbeek F, Parizel P, Bellemans J (2009) A common reference frame for describing rotation of the distal femur: A CT-based kinematic study using cadavers. J Bone Joint Surg 91-B(5):683–690
25. Wu G, Siegler S, Allard P, Kirtley C, Leardini A, Rosenbaum D, Whittle M, D'Lima DD, Cristofolini L, Witte H, Schmid O, Stokes I (2002) ISB recommendation on definitions of joint coordinate system of various joints for the reporting of human joint motion part I: ankle, hip, and spine. J Biomech 35(4):543–548